**8b** (5 equiv of NaI, 100 °C, 1 h) which gave **10b**[6] as the sole cyclic product.

In summary, the possibility to tune the reactivity of alkynes by external nucleophiles opens up new opportunities for the use of this readily available functional group. Our ongoing studies aim at extending nucleophile-promoted alkyne cyclizations to other initiating cations and ring sizes as well as providing some definition of the mechanism[18] of these transformations.

**Acknowledgment.** This investigation was supported by NIH Grant HL-25854 and by Shared Instrument Grants from the National Science Foundation.

**Supplementary Material Available:** Experimental procedures and characterization data for representative cyclic products **2a–d**, **4a**, **5a**, **5c**, **6b**, **7**, **9**, and **10a** are provided (7 pages). Ordering information is given on any current masthead page.

(18) One possibility, which is suggested by our recent mechanistic study[5] of iminium ion–alkene cyclizations, would involve rate-determining attack of a nucleophile on a $\pi$-complex (or bridged cation) produced from reversible interaction of the iminium ion and alkyne groups.

## Simulation of Crystal Structures by Empirical Atom–Atom Potentials. 2. The Orthorhombic-to-Tetragonal Phase Transition in the High-Temperature ($T_c$ > 90 K) Superconductor $YBa_2Cu_3O_{7-y}$

Michel Evain and Myung-Hwan Whangbo*

*Department of Chemistry*
*North Carolina State University*
*Raleigh, North Carolina 27695-8204*

Mark A. Beno and Jack M. Williams*

*Chemistry and Materials Science Divisions*
*Argonne National Laboratory*
*Argonne, Illinois 60439*

*Received June 25, 1987*

It is well established from several powder neutron diffraction studies[1] that the Y–Ba–Cu–O phase with the superconducting transition temperature ($T_c$) greater than 90 K[2] is orthorhombic $YBa_2Cu_3O_{7-y}$ ($y \simeq 0.19$). The important structural unit of this phase is the $Ba_2Cu_3O_{7-y}^{3-}$ slab.[1,3] which consists of two $CuO_2$ layers that sandwich one $CuO_3$ chain and two $Ba^{2+}$ cations per unit cell (see Figure 1). The copper atoms (Cu2) of the $CuO_2$ layers are linked to the copper atoms (Cu1) of the $CuO_3$ chains via the capping oxygen atoms (O4). Band electronic structure studies[3] reveal that the $CuO_2$ layers of each $Ba_2Cu_3O_{7-y}^{3-}$ slab interact via the Cu2–O4–Cu1–O4–Cu2 linkages. Upon increasing temperature in a pure oxygen atmosphere, $YBa_2Cu_3O_{7-y}$ gradually loses the oxygen atoms O1 of the Cu1 atom planes thereby destroying the $CuO_3$ chains[4a] and eventually undergoes an orthorhombic to tetragonal phase transition near ~1000 K.[4a] which occurs when the stoichiometry of $YBa_2O_{7-y}$ is close to $YBa_2Cu_3O_{6.5}$.[4a]

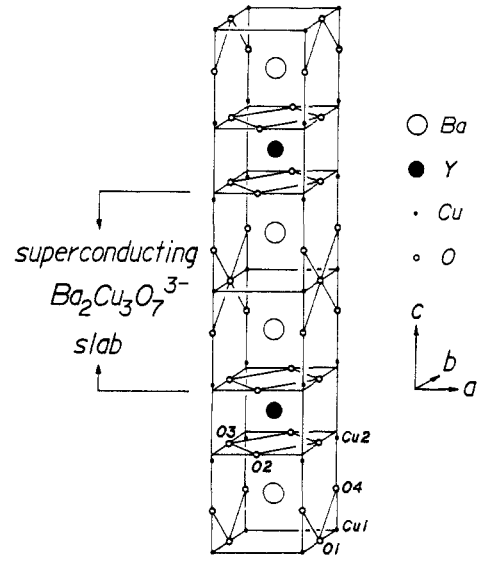


**Figure 1.** Crystal structure of $YBa_2Cu_3O_{7-y}$ ($y \simeq 0.19$) determined by neutron diffraction.[1a]

**Table I.** The Atom–Atom Potential Parameters for $Ba^{2+}\cdots Ba^{2+}$ and $Y^{3+}\cdots Y^{3+}$

| pair | $B$ (eV) | $\rho$ (Å) | $C$ (eV. Å$^6$) |
|---|---|---|---|
| $Ba^{2+}\cdots Ba^{2+}$ | 3749.5 | 0.350 | 442.1 |
| $Y^{3+}\cdots Y^{3+}$ | 6902.5 | 0.250 | 18.44 |

An important structural change in $YBa_2Cu_3O_{7-y}$ induced by increasing the O1 atom vacancies is a Cu1–O4 distance shortening and a Cu2–O4 distance elongation (e.g., Cu1–O4 = 1.850 (3) and 1.800 (6) Å, and Cu2–O4 = 2.303 (3) and 2.486 (10) Å for $YBa_2Cu_3O_{6.81}$[1a] and $YBa_2Cu_3O_{6.42}$,[4a] respectively). Thus an increase in the O1 atom vacancies lenghtens the Cu2–O4–Cu1–O4–Cu2 linkages.

Another structural aspect of importance in $YBa_2Cu_3O_{7-y}$ is the gradual increase in the length of the unit cell $c$ parameter with increasing temperature, which is *not* a simple thermal expansion: The $c$ parameter, the $Ba^{2+}\cdots Ba^{2+}$ distance, and the $Ba^{2+}\cdots Y^{3+}$ distance are, respectively, 11.6807 (2), 4.306 (7), and 3.688 (3) Å for orthorhombic $YBa_2Cu_3O_{6.81}$ at room temperature,[1a] while they are, respectively, 11.9403 (5), 4.607 (7), and 3.685 (3) Å for tetragonal $YBa_2Cu_3O_{6.42}$ at 1091 K.[4a] The $Ba^{2+}\cdots Y^{3+}$ distance remains nearly constant, so that the increase in the $c$ parameter is nearly equal to that in the $Ba^{2+}\cdots Ba^{2+}$ distance.[4a] In fact, with increasing temperature, the $Ba^{2+}$ cations move farther away from the Cu1 atom planes.[4a,5] Even when the room temperature

(1) (a) Beno, M. A.; Soderholm, L.; Capone, D. W., II; Hinks, D. G.; Jorgensen, J. D.; Schuller, I. K.; Segre, C. U.; Zhang, K.; Grace, J. D. *Appl. Phys. Lett.* **1987**, *51*, 57. (b) Greedan, J. E.; O'Reilly, A.; Stager, C. V. *Phys. Rev. B: Condens. Matter* **1987**, *37*, 8770. (c) Capponi, J. J.; Chaillout, C.; Hewart, A. W.; Lejay, P.; Marezio, M.; Nguyen, N.; Raveau, B.; Soubeyroux, J. L.; Tholence, J. L.; Tournier, R. *Europhys. Lett.* **1987**, *3*, 1301. (d) David, W. I. F.; Harrison, W. T. A.; Gunn, J. M. F.; Moze, O.; Soper, A. K.; Day, P.; Jorgensen, J. D.; Beno, M. A.; Capone D. W., II; Hinks, D. G.; Schuller, I. K.; Soderholm, L.; Segre, C. U.; Zhang, K.; Grace, J. D. *Nature (London)* **1987**, *327*, 310. (e) Beech, F.; Miraglia, S.; Santoro, A.; Roth, R. S. *Phys. Rev. B: Condens. Matter* **1987**, *35*, 8770. (f) Katano, S.; Funahasi, S.; Hatano, T.; Matsushita, A.; Nakamura, K.; Matsumoto, T.; Ogawa, K. *Jpn. J. Appl. Phys., Part 2* **1987**, *26*, L1046. (g) Cox, D. E.; Moodenbaugh, A. R.; Hurst, J. J.; Jones, R. H. *J. Phys. Chem. Solids*, submitted for publication.

(2) (a) Wu, M. K.; Ashburn, J. R.; Torng, C. J.; Hor, P. H.; Meng, R. L.; Gao, L.; Huang, Z. J.; Wang, Y. Q.; Chu, C. W. *Phys. Rev. Lett.* **1987**, *58*, 908. (b) Hinks, D. G.; Soderholm, L.; Capone D. W., II; Jorgensen, J. D.; Schuller, I. K.; Segre, C. U.; Zhang, K.; Grace J. D. *Appl. Phys. Lett.* **1987**, *50*, 1688. (c) Cava, R. J.; Batlogg, B.; van Dover, R. B.; Murphy, D. W.; Sunshine, S.; Siegrist, T.; Remeika, J. P.; Reitman, E. A.; Zahurak, S.; Espinosa, G. P. *Phys. Rev. Lett.* **1987**, *58*, 1676. (d) Grant, P. M.; Beyers, R. B.; Engler, E. M.; Lim, G.; Parkin, S. P.; Ramirez, M. L.; Lee, V. Y.; Nazzal, A.; Vazquez, J. E.; Savoy, R. J. *Phys. Rev. B: Condens. Matter* **1987**, *35*, 7242. (e) Syono, Y.; Kikuchi, M.; Oh-ishi, K.; Hiraga, K.; Arai, H.; Matsui, Y.; Kobayashi, N.; Sasoka, T.; Moto, Y. *Jpn. J. Appl. Phys.* **1987**, *26*, L498. (f) Hazen, R. M.; Finger, L. W.; Angel, R. J.; Prewitt, C. T.; Ross, N. L.; Mao, H. K.; Hadidiacos, C. G.; Hor, P. H.; Meng, R. L.; Chu, C. W. *Phys. Rev. B: Condens. Matter* **1987**, *35*, 7238.

(3) (a) Whangbo, M.-H.; Evain, M.; Beno, M. A.; Williams, J. M. *Inorg. Chem.* **1987**, *26*, 1831. (b) Whangbo, M.-H.; Evain, M.; Beno, M. A.; Williams, J. M. *Inorg. Chem.* **1987**, *26*, 1832.

(4) (a) Jorgensen, J. D.; Beno, M. A.; Hinks, D. G.; Soderholm, L.; Volin, K. J.; Hitterman, R. L.; Grace, J. D.; Schuller, I. K.; Segre, C. U.; Zhang, K.; Kleefisch, M. S. *Phys. Rev. B: Condens. Matter* **1987**, *36*, 3608. (b) Santoro, A.; Miraglia, S.; Beech, F.; Sunshine, S. A.; Murphy, D. W.; Schneemeyer, L. F.; Waszczak, J. V. *Mat. Res. Bull.* **1987**, *22*, 1007. (c) Katano, S.; Funahashi, S.; Hatano, T.; Matsushita, A.; Nakamura, K.; Matsumoto, T.; Ogawa, K. *Jpn. J. Appl. Phys., Part 2* **1987**, *26*, L1049.

0002-7863/88/1510-0614$01.50/0 

**Table II.** The Experimental and Calculated Values for the Unit Cell and Atom Positional Parameters of BaO, $Y_2O_3$, Orthorhombic $YBa_2Cu_3O_{7-y}$, and Tetragonal $YBa_2Cu_3O_{7-y}$[a,b]

| BaO | $Y_2O_3$ | $YBa_2Cu_3O_7$[c] | $YBa_2Cu_3O_{6.5}$[d] |
|---|---|---|---|
| cubic | cubic | orthorhombic | tetragonal |
| (NaCl) | (*Ia*3) | (*Pmmm*) | (*P*4/*mmm*) |
| $a$ = 5.523 (0.000) | $a$ = 10.604 (0.020) | $a$ = 3.8231 (0.1092) | $a$ = 3.9018 (0.0530) |
| | | $b$ = 3.8863 (−0.0428) | $c$ = 11.9403 (0.0350) |
| | $x$(Y2) = −0.0314 (0.0017) | $c$ = 11.6809 (0.1040) | |
| | $x$(O) = 0.389 (0.003) | | $z$(Ba) = 0.1914 (0.0002) |
| | $y$(O) = 0.150 (0.004) | $z$(Ba) = 0.1843 (0.0036) | $z$(Cu2) = 0.3590 (−0.0016) |
| | $z$(O) = 0.377 (0.005) | $z$(Cu2) = 0.3556 (−0.0192) | $z$(O2) = 0.3792 (0.0006) |
| | | $z$(O2) = 0.3773 (−0.0012) | $z$(O4) = 0.1508 (−0.0203) |
| | | $z$(O3) = 0.3789 (−0.0028) | |
| | | $z$(O4) = 0.1584 (0.0074) | |

[a] Experimental values are the numbers without parentheses. The numbers in the parentheses refer to the deviations of the calculated values from the corresponding experimental ones. [b] The unit cell parameters are in units of Å. [c] The experimental values are taken from orthorhombic $YBa_2Cu_3O_{6.81}$.[1a] [d] The experimental values are taken from tetragonal $YBa_2Cu_3O_{6.42}$.[4a]

structure of orthorhombic $YBa_2Cu_3O_{6.81}$[4a] and tetragonal $YBa_2Cu_3O_{6.06}$[4b] are compared, it is still true that the Cu1–O4 distance is shorter, while the $c$ parameter, the $Ba^{2+}\cdots Ba^{2+}$, and the Cu2–O4 distances are greater, in the tetragonal phase. In the present study, we analyze these structural features by performing empirical atom–atom potential[6] calculations as employed in our previous work (part 1)[7] on $La_2CuO_4$ and discuss their implications concerning the two plateaus in the $T_c$ vs oxygen content plot for $YBa_2Cu_3O_{7-y}$ (i.e., $T_c \simeq 93$ K for $y \simeq 0.15$–$0.25$; $T_c \simeq 55$ K for $y \simeq 0.40$–$0.50$).[5,8]

By using the WMIN program of Busing[9] together with the $B$, $\rho$, and $C$ values derived for the $O^{2-}\cdots O^{2-}$ pair in part 1, we determine[10] the corresponding values for the $Ba^{2+}\cdots Ba^{2+}$ and $Y^{3+}\cdots Y^{3+}$ pairs that reproduce the crystal structures of BaO[11] and $Y_2O_3$,[12] respectively. Listed in Table I are the $B$, $\rho$, and $C$ values thus obtained, which describe very well the unit cell and atom positional parameters of BaO and $Y_2O_3$ as summarized in Table II. In our WMIN calculations on $YBa_2Cu_3O_{7-y}$, the orthorhombic and tetragonal phases are represented by the ideal compositions $YBa_2Cu_3O_7$ and $YBa_2Cu_3O_{6.5}$, respectively. As already noted, copper atoms with different oxidation states are present in orthorhombic and tetragonal $YBa_2Cu_3O_{7-y}$.[3,14] In principle, different sets of $B$, $\rho$, and $C$ values might be derived for different copper atoms, but this is impractical due to lack of appropriate copper oxides from which to refine different sets of parameters. Since we are mainly interested in qualitative changes between the orthorhombic and tetragonal structures, we use the $B$, $\rho$, and $C$ values derived for the $Cu^{2+}\cdots Cu^{2+}$ pair in part 1 for all copper···copper pairs of $YBa_2Cu_3O_{7-y}$. Then, the average oxidation states of +2.3333 and +2 may be used for the copper atoms of orthorhombic $YBa_2Cu_3O_7$ and tetragonal $YBa_2Cu_3O_{6.5}$, respectively. The partial occupancy (0.25) of the O1 atom sites in tetragonal $YBa_2Cu_3O_{6.5}$ may be simulated by assuming that all the O1 atom sites are fully occupied (1.0) but that the atom–atom potentials[6] associated with each O1 atom are reduced by a factor of four per O1. With these approximations, we calculate the crystal energies of orthorhombic $YBa_2Cu_3O_7$ and tetragonal $YBa_2Cu_3O_{6.5}$ as a function of their unit cell and atom positional parameters and thus obtain their calculated optimum crystal structures.

As summarized in Table II, the calculated and the experimental crystal structures are in good agreement for both orthorhombic and tetragonal $YBa_2Cu_3O_{7-y}$.[15] The present calculations correctly predict that the Cu1–O4 distance is shorter, while the $c$ parameter, the Cu2–O4, and the $Ba^{2+}\cdots Ba^{2+}$ distances are all greater in the tetragonal phase. These results originate from the anisotropic oxygen atom environment around each $Ba^{2+}$ cation: For orthorhombic and tetragonal $YBa_2Cu_3O_{7-y}$, the Cu2 atom plane has more $O^{2-}$ anions than does the Cu1 atom plane. Thus, the Coulomb attraction of the $Ba^{2+}$ cation is stronger with the Cu2 atom plane. As the O1 atoms are gradually lost upon increasing temperature,[4a] the Coulomb attraction of the $Ba^{2+}$ cation and the Coulomb repulsion of the capping oxygen atom O4 with the $O^{2-}$ anions of the Cu1 atom plane are gradually weakened. Consequently, the O4 atom comes closer to, but the $Ba^{2+}$ cation moves farther away from, the Cu1 atom plane.

To summarize, the oxygen atom environment of the $Ba^{2+}$ cation is anisotropic in orthorhombic $YBa_2Cu_3O_{7-y}$, the extent of which increases upon increasing temperature due to the preferential loss of the oxygen atoms O1. With increasing the O1 atom vacancies, the Cu2–O4–Cu1–O4–Cu2 linkages are elongated thereby weakening the interaction between the $CuO_2$ layers in each $Ba_2Cu_3O_{7-y}^{3-}$ slab. Upon reducing this interlayer interaction, the $CuO_2$ layers may act independently as in the case of the $CuO_4$ layers in $La_{2-x}M_xCuO_4$.[7] Thus, it is suggested that the lower plateau of the $T_c$ vs oxygen content plot for $YBa_2Cu_3O_{7-y}$ (i.e., $T_c \simeq 55$ K for $y \simeq 0.40$–$0.50$)[5,8] occurs when the $CuO_2$ layers of each $Ba_2Cu_3O_{7-y}^{3-}$ slab are electronically decoupled, while the upper plateau (i.e., $T_c \simeq 93$ K for $y \simeq 0.15$–$0.25$)[5,8] occurs when the $CuO_2$ layers are electronically coupled via the Cu2–O4–Cu1–O4–Cu2 linkages.[3b]

**Acknowledgment.** Work at North Carolina State University and Argonne National Laboratory was supported by the U.S. Department of Energy, Office of Basic Energy Sciences, Division of Materials Sciences under Grant DE-FG05-86-ER45259 and under Contract W31-109-ENG-38, respectively. We express our

(5) Whangbo, M.-H.; Evain, M.; Beno, M. A.; Geiser, U.; Williams, J. M. *Inorg. Chem.*, in press.
(6) (a) Stoneham, A. M.; Harding, J. H. *Ann. Rev. Phys. Chem.* **1986**, *37*, 53. (b) *Computer Simulation of Solids*; Catlaw, C. R. A., Mackrodt, W. C., Eds.; Springer-Verlag: New York, 1982. (c) Williams, D. E. *Top. Curr. Phys.* **1981**, *26*, 3. (d) Mirsky, K. *In Computing in Crystallography*; Delft University Press: Twente, 1978; p 169.
(7) Evain, M.; Whangbo, M.-H.; Beno, M. A.; Geiser, U.; Williams, J. A., *J. Am. Chem. Soc.* in press (previous paper, part 1).
(8) (a) Veal, B. W.; Jorgensen, J. D.; Crabtree, G. W.; Kwok, W.; Umezawa, A.; Paulikas, A. P.; Morss, L. R.; Appelman, E. H.; Nowicki, L. J.; Nuñez, L.; Claus, H. *International Conference on Electronic Structure and Phase Stability in Advanced Ceramics*; August 17–19, 1987; Argonne National Laboratory: Argonne, IL. (b) Johnston, D. C.; Jacobson, A. J.; Newsam, J. M.; Lewandowski, J. T.; Goshorn, D. P.; Xie, D.; Yelon, W. B. *Symposium on Inorganic Superconductors*; National Meeting of the American Chemical Society; August 31–September 4, 1987; New Orleans, LA.
(9) Busing, W. R. "WMIN, *A Computer Program To Model Molecules and Crystals in Terms of Potential Energy Functions*; Oak Ridge National Laboratory, Oak Ridge, TN, 1981, ORNL-5497.
(10) We refined the $B$ and $\rho$ parameters of the $Ba^{2+}\cdots Ba^{2+}$ and $Y^{3+}\cdots Y^{3+}$ pairs on the basis of the work on $Ba^{2+}\cdots O^{2-}$ and $La^{3+}\cdots O^{2-}$.[7,13]
(11) Zollweg, R. J. *Phys. Rev.* **1955**, *100*, 671.
(12) O'Conner, B. H.; Valentine, T. M. *Acta Crystallogr., Sect. B: Struct. Crystallogr. Cryst. Chem.* **1969**, *B25*, 2140.
(13) (a) Stoneham, A. M. *Handbook of Interaction Potentials, Vol. 1, Ionic Crystals*; Didicot: AERE Harwell, Rep., AERE-R 9598, 1979; p 102. (b) Mackrodt, W. C.; Steward, R. F. *J. Phys.* **1979**, *C12*, 431.
(14) Whangbo, M.-H.; Evain, M.; Beno, M. A.; Geiser, U.; Williams, J. M. *Inorg. Chem.* **1987**, *26*, 2566.

(15) The calculated structure for orthorhombic $YBa_2Cu_3O_7$ represents a saddle point on the eight-dimensional potential energy surface. With the present set of empirical potentials, any minimum energy structure calculated for orthorhombic $YBa_2Cu_3O_7$ is found physically meaningless.

appreciation for computing time made available by DOE on the ER-Cray X-MP computer. We are grateful to Dr. W. R. Busing for making his WMIN program available to us and to Dr. D. Wolf for references.

## Natural Abundance Deuterium NMR as a Novel Probe of Monoterpene Biosynthesis: Limonene

M. F. Leopold, William W. Epstein,* and David M. Grant*

*Department of Chemistry, University of Utah*
*Salt Lake City, Utah 84112*
*Received June 8, 1987*

Our interest in proton-decoupled, natural abundance deuterium nuclear magnetic resonance spectroscopy ($^2$H NMR) of monoterpenes has been sparked by the observation that at natural abundance, deuterium resonances of natural camphor-*d* have markedly different relative peak intensities compared to the proton spectrum and that these intensities are different from those observed for synthetic camphor (derived from α-pinene).[1] Although the first natural abundance $^2$H NMR spectrum of *n*-butyl iodide was obtained in 1973,[2] experimental considerations have prevented its commonplace use (compared with $^{13}$C NMR). However, the advent of modern high field NMR technology coupled with short $T_1$'s (<7 s)[3] and negligible NOE's now allows measureable differences in deuterium peak intensities to be directly related to $^2$H/$^1$H ratios at specific sites in a molecule. Thus, deuterium at natural abundance is the "perfect" isotopic tracer since no synthesis of labeled substrate is required and individual site-specific differences can be measured.

Martin et al. first noted that at natural abundance large variations in site-specific $^2$H/$^1$H ratios occurred and that these integration values varied greatly from synthetic to naturally derived compounds. Both ethanol[5] and anethole[6,7] were found to have different identifiable $^2$H/$^1$H site-specific ratios related to source of origin. More recently, primary KIE's of several well-understood reactions have been measured by using natural abundance $^2$H NMR, and $k_H/k_D$ values were comparable with literature values.[8] Analysis of α- and β-pinene suggested that isotopically sensitive partitioning within the pinene cyclase enzyme was occurring[8] and the measured KIE was similar to the theoretical value for such a partitioning.[9] A correlation between the optical purity and site-specific deuterium hydrogen ratios has been observed for α-pinene as well.[10]

Our study of monoterpene biosynthesis led us to select limonene (**4**), the simplest of the *p*-menthane monoterpenes, for analysis since the question of the genesis of the exocyclic double bond has not been satisfactorily answered experimentally. A shortened form of the proposed biosynthesis of limonene is shown in Scheme I.[11] Generation of this olefin required only proton loss from the α-terpinyl cation **3** postulated as a common intermediate in many bicyclic monoterpene biosyntheses. Although both C-7 and C-9 of **2** are derived from the methyl group of mevalonic acid (**1**)[12] and proton loss to form limonene is postulated to be regiospecific

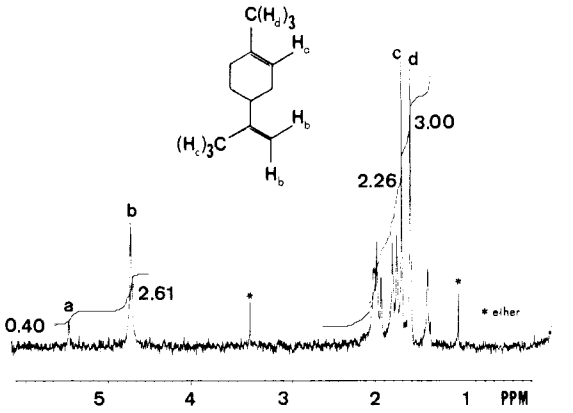


**Figure 1.** Natural abundance, proton-decoupled $^2$H NMR spectrum (61.4 MHz) of *R*-(+)-limonene. The impurity marked is ethyl ether used in extraction. The 2 M solution was prepared with $C_6F_6$ as the lock solvent and TMS as the chemical shift reference. The acquisition parameters used were as follows: acquisition time, 3 s; pulse width, 80°; number of transients, 10 000; probe temperature, 30 °C.

**Scheme I**

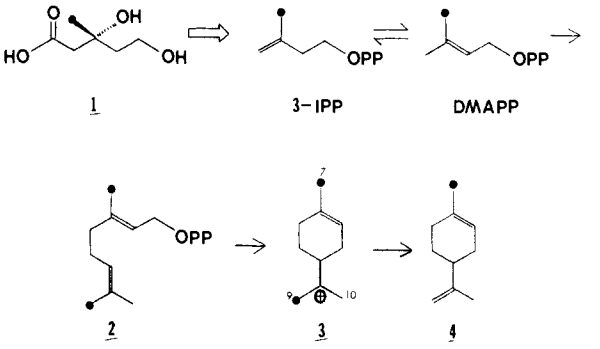


from C-9 of **3**, tracer studies of incorporation of 2-$^{14}$C mevalonic acid were far from conclusive.[13] Analysis of a more recent feeding study using [4.10-$^3$H$_4$,U-$^{14}$C]geraniol has suggested that proton abstraction occurs only from C-9, but incorporation was low and apparently not reproducible.[14]

Natural *R*-(+)-limonene was isolated by steam distillation followed by ether extraction from Florida navel oranges collected exclusively from one tree. The purity of this sample was assessed by $^1$H NMR and GC and found to be >98%; the measured optical rotation was $[\alpha]^{21}_D = 96.6°$ (neat). Selective $^1$H-$^1$H decoupling experiments allowed assignment of the two methyls in the proton spectrum. This assignment is analogous in the natural abundance deuterium spectrum shown in Figure 1. The integrated intensity of the methyl hydrogens of C-7 is used as an internal standard for normalization since this methyl group remains unperturbed throughout the biosynthesis.[8] A relative depletion of 25% (2.26) is observed for the isopropenyl methyl hydrogens, $H_c$, relative to the hydrogens, $H_d$, of C-7. This depletion is clearly inconsistent with selective loss of a proton from C-10. If proton loss had occurred regiospecifically from C-10, then the integrated intensities of the methyl groups should be the same within experimental error.[15] This is not the case, and the relative depletion of deuterium noted in the isopropenyl methyl hydrogens can be directly traced to the 3-isopentylpyrophosphate (IPP) → dimethylallylpyrophosphate (DMAPP) isomerization.

The isopropenyl vinyl hydrogens, $H_b$, are enhanced to a relative value of 2.61 ± 0.13 (statistically this value should be 2 in the absence of any KIE). The enhancement of the isopropenyl vinyl hydrogens is expected since hydrogen abstraction is favored over deuterium abstraction, and $k_H/k_D$ may be calculated from eq 1

(1) Grant, D. M.; Curtis, J.; Croasmun, W. R.; Dalling, D. K.; Wehrli, F. W.; Wehrli, S. *J. Am. Chem. Soc.* **1982**, *104*, 4492.
(2) Briggs, J. M.; Farnell, L. F.; Randall, E. W. *J. Chem. Soc., Chem. Commun.* **1973**, 70.
(3) Mantsch, H. H.; Saito, H.; Smith, I. C. P. *Prog. NMR Spectrosc.* **1977**, *11*, 211.
(4) Martin, G. J.; Martin, M. L. *Tetrahedron Lett.* **1981**, *22*, 3525.
(5) Martin, G. J.; Martin, M. L.; Mabon, F.; Michon, M.-J. *J. Agric. Food Chem.* **1983**, *31*, 311.
(6) Martin, G. J.; Martin, M. L.; Malbon, F. *J. Am. Chem. Soc.* **1982**, *104*, 2658.
(7) Martin, G. J.; Javier, P.; Mabon, F. *Analusis* **1985**, *13*, 267.
(8) Pascal, R. A.; Baum, M. W.; Wagner, C. K.; Rodgers, L. R.; Huang, D. *J. Am. Chem. Soc.* **1986**, *108*, 6477.
(9) Jones, J. P.; Korzekwa, K. R.; Rettie, A. E.; Trager, W. F. *J. Am. Chem. Soc.* **1986**, *108*, 7074.
(10) Martin, G. J.; Janvier, P.; Akoka, S.; Mabon, F.; Jurczak, J. *Tetrahedron Lett.* **1986**, *27*, 2855.
(11) Croteau, R. B. *Chem. Rev.* **1987**, *87*, 929.
(12) Cornforth, J. W. *Tetrahedron* **1974**, *30*, 1515.
(13) Sandermann, W.; Bruns, K. *Planta Medica* **1965**, *13*, 364.
(14) Akhila, A.; Banthorpe, D. V.; Rowan, M. G. *Phytochem.* **1980**, *19*, 1433.
(15) Analytical studies in this laboratory have determined the experimental error for deuterium integration is 5%.

0002-7863/88/1510-0616$01.50/0 